

# MEASUREMENT OF TRANSVERSE STATISTICAL DEPENDENCE FOR NON-GAUSSIAN BEAM DISTRIBUTIONS VIA RESONANCES IN THE CERN PSB

E. Lamb<sup>\*1</sup>, F. Asvesta, H. Bartosik, G. Sterbini, CERN, Geneva, Switzerland  
<sup>1</sup>also at EPFL, Lausanne, Switzerland

## Abstract

Non-Gaussian heavy-tail transverse beam profiles can be used to reconstruct the 4D beam distribution in phase space under two different conditions, that is independent or dependent distribution functions across the  $x$ - $y$ -plane. The two conditions lead to different implications for the physics of the beam. In the case of dependent distributions, this results in profile changes in one plane through a loss process on the other. This work explores how different resonances, either 1D or 2D can lead to tail population with statistical dependence. Original measurements performed in the Proton Synchrotron Booster at the CERN accelerator complex demonstrate this effect and are hereby presented and discussed.

## INTRODUCTION

We often observe heavy-tail non-Gaussian beam profiles in the CERN accelerator complex at the LHC [1] and in the injectors [2]. For luminosity studies in the LHC, but also for scenarios involving loss mechanisms, it is interesting to reconstruct the most realistic particle distribution corresponding to the profile observed.

We define a normalised phase space, for a linear machine, via a transformation:

$$\begin{bmatrix} 1/\sqrt{\beta_x} & 0 \\ \alpha_x/\sqrt{\beta_x} & \sqrt{\beta_x} \end{bmatrix} \begin{bmatrix} x_1 & p_{x1} \\ x_2 & p_{x2} \\ \dots & \dots \end{bmatrix}^T \quad (1)$$

yielding a rotationally symmetric  $x$ - $p_x$  phase space, where  $\alpha_x$ ,  $\beta_x$  are the machine optics functions. The equivalent is true in the  $y$  plane. We define the normalised profile in one of the transverse planes ( $x$ ,  $y$ ) as an integration of a 4D ( $x$ ,  $p_x$ ,  $y$ ,  $p_y$ ) distribution function in the other three planes, e. g. for the horizontal plane:

$$f_{1D}(x) = \iiint f_{4D}(x, p_x, y, p_y) dp_x dy dp_y. \quad (2)$$

To reconstruct the probability density function  $f_{4D}(x, p_x, y, p_y)$  of the matched distribution there is a constraint that in the normalised  $x$ - $p_x$  and  $y$ - $p_y$  phase space, the beam is rotationally symmetric. To reconstruct the 2D distribution functions  $f_{2D}(x, p_x)$  and  $f_{2D}(y, p_y)$ , we can use a form of the inverse Abel transform [3, 4], of which the ‘inverse’ transform is given by:

$$f_{2D}(r) = -\frac{1}{\pi} \int_r^\infty \frac{df_{1D}(x)}{dx} \frac{dx}{\sqrt{x^2 - r^2}}, \quad (3)$$

where  $r^2 = x^2 + p_x^2$ , which transforms the 1D profile projection to a 2D distribution under this constraint. To find the 4D phase space distribution, there are not enough constraints, thus there are infinite distributions with the same 1D projection (for the non-Gaussian case). We show two examples, one forming  $f_{4D}$  assuming independent distributions in  $x$  and  $y$ , and the other using a constraint that the beam is rotationally symmetric also in the normalised  $x$ - $y$ -plane.

Choosing independent, or factorisable distributions, we generate the 4D particle distribution function (PDF)

$$f_{4D}(x, p_x, y, p_y) = f_{2D}(x, p_x) \times f_{2D}(y, p_y). \quad (4)$$

This results in a ‘cross’-shaped beam in the  $x$ - $y$ -space for heavy tailed profiles, as can be seen in Fig. 1 (top), using the example of a  $q$ -Gaussian [5] with  $q$ -parameter 1.4.

Alternatively, to reconstruct  $f_{4D}$  assuming rotational symmetry in the  $x$ - $y$ -plane, we use a series of inverse Abel transforms, exploiting the property that they can find higher dimensional distributions as long as they are axisymmetric. Then, the full distribution is populated via a Box-Müller type random 4D generator [6, 7]. Figure 1 (bottom) shows the rotationally symmetric distribution, which gives the same 1D projection, or ‘profile’ as the other method.

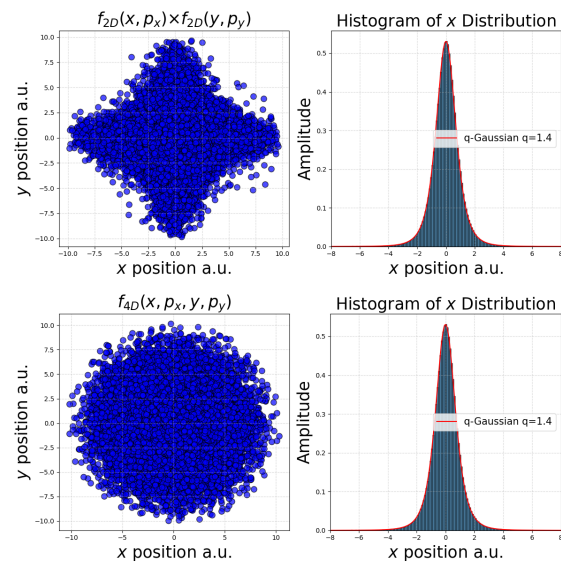


Figure 1: A heavy tailed beam generated in normalised phase space with two methods, giving the same projection on the  $x$  (and  $y$ ) plane and matched distributions in a linear and uncoupled lattice: factorisable distributions (top) and assuming rotational symmetry in the  $x$ - $y$ -plane (bottom).

\* elamb@cern.ch

It should be noted that the two extreme methods are equivalent for Gaussian distributions, as the inverse Abel transform of a Gaussian is a Gaussian. However, for non-Gaussian distributions, there are different physical consequences of how the distribution behaves under loss mechanisms.

Figure 2 shows the covariance matrices for the rotationally-symmetric PDF generated with different numbers of particles. In both cases there is no coupling between the  $x$  and  $y$  distributions beyond the numerical noise, which decreases with particle number increase. However there is statistical dependence between the two planes.

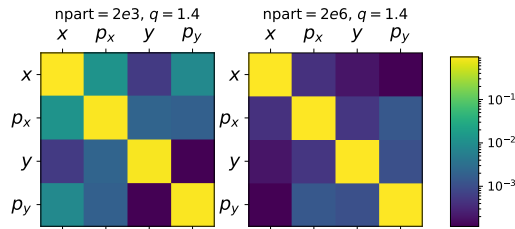


Figure 2: The covariance matrices of a 4D beam distribution numerically generated with dependent PDFs for  $2 \times 10^3$  particles (left) and  $2 \times 10^6$  particles (right).

In fact, as shown in Fig. 3 (bottom), when particles are shaved in the horizontal plane, (e. g., removing particles with  $x^2 + p_x^2 > r_0^2$ ), the  $y$ -plane profile changes due to the non-factorisable PDF. On the other hand, this effect is not observed for beams featuring the cross-shaped distribution in  $x$ - $y$  obtained for factorisable PDFs, as shown in Fig. 3 (top).

It is unclear which type of distribution is the most physical for beams with heavy tails. This can have an impact on the luminosity calculation, as it is usually done assuming independent probability density functions [8]. Non-factorisation of the  $x$ - $y$ -plane was suggested as a reason for uncertainty in the Van De Meer scans by ATLAS [9]. Furthermore, the lifetime prediction can be affected, as the losses depend on the full beam distribution, which is unknown.

The goal of the paper is to find the experimental beam distributions resulting from the controlled beam interaction with 1D and 2D resonances in the presence of space charge, a typical scenario encountered in the injectors of the LHC accelerator chain. Furthermore, the aim is to see if the dependence is present on the horizontal plane when shaving the beam in the vertical plane.

## EXPERIMENTAL PROCEDURE

An experiment was proposed to demonstrate the effect of the statistical dependence between the planes, by subjecting a bunched beam to 1D and coupled 2D resonances in the Proton Synchrotron Booster (PSB) in the presence of space charge. Due to fixed line structures of 2D coupled resonances periodically crossing the particle distribution [10], a halo will be populated [11]. The distribution of the halo will be

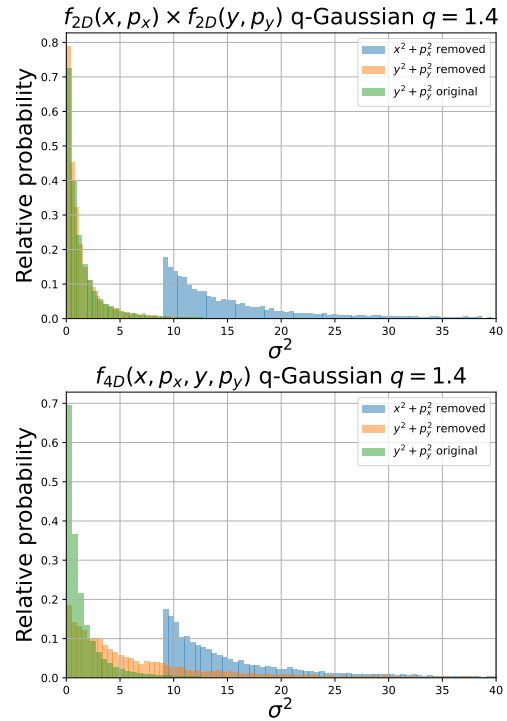


Figure 3: The change in distribution when particles are 'collimated' in one transverse plane for two different types of 4D PDFs.

different in the transverse planes. The hypothesis is that the fixed line structures induce dependence in the  $x$ - $y$ -planes via a more likely amplitude in  $x$  for a given  $y$ , which remains present even when the particles are no longer exposed to the resonance since the beam is never 'mismatched'. In contrast, a 1D resonance should not introduce dependence between the planes. The tails are shaved in the vertical plane (V) where there is no dispersion, and the beam profile in the horizontal plane (H) is measured. With no dependence, the normalised profile w.r.t intensity will be unaffected in H.

The measurements were carried out in Ring 1 of the PSB at injection energy  $E_k = 160$  MeV, and the beam is stored for  $\approx 400$  ms. A low intensity bunch with  $50 \times 10^{10}$  protons was used in order to reduce the space charge tune-spread so that only one resonance at the time is crossing the particle distribution, making it easier to excite the lattice resonances in a controlled way. The beam's momentum spread was reduced to  $1 \times 10^{-3}$ , to remove as much as possible the chromatic effects from the beam profiles, as there is no horizontal zero dispersion region in the PSB.

Two resonances were investigated, the  $3Q_y = 13$ , a 1D third order skew resonance, and  $Q_x + 2Q_y = 13$ , a 2D third order normal resonance. For each resonance, the bare machine working point was placed at a distance from the resonance line to maximise tail population but minimise losses. The working points were further optimised to be far from other resonance lines. The machine resonances for Ring 1 in the vicinity of the working point were corrected using compensation schemes derived in previous experiments [12]. Figure 4

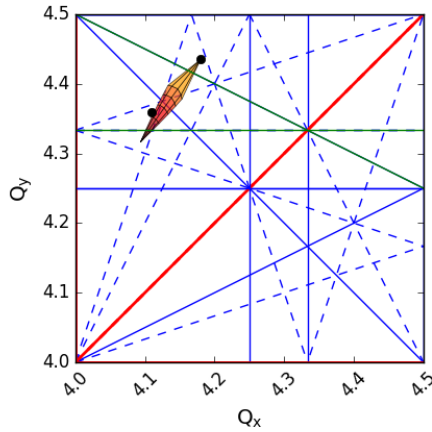


Figure 4: Space charge tune shift and the working point for both resonances, which are highlighted in green.

shows the tune diagram with all resonances plotted up to 4<sup>th</sup> order, with the two resonances of interest highlighted in green. The tune-spread, shown by the necktie, was estimated using PySCRDT [13], and the bare machine working points used in the experiment are shown by the black dots, i. e. for  $3Q_y = 13$ ,  $(Q_x, Q_y) = (4.11, 4.36)$  and for  $Q_x + 2Q_y = 13$ , at  $(Q_x, Q_y) = (4.18, 4.44)$ .

The low intensity beam is injected from LINAC4 at 275 ms. The chosen resonance is artificially excited with a skew or normal sextupole from 350 ms to 550 ms, thus after transients from the injection process have occurred [14]. After the removal of the resonance excitation, the beam is shaved at 590 ms, via a vertical closed orbit bump towards a fixed beam absorber. The beam profile is measured with the wire scanners at 600 ms. Horizontal or vertical profiles are measured in alternate cycles. The shaved intensity is varied between 0% and around 45% of the total. At least five measurements are taken for each setting. Longitudinal profiles were also measured using the tomoscope for reconstruction via tomography [15], but are not discussed here.

## RESULTS

Figure 5 shows wire scanner profiles and Figs. 6 and 7 show the aggregated results. In both cases, a  $q$ -Gaussian [5] was fitted to the profile measurement in the two transverse planes. If the  $q$ -parameter  $> 1$ , the beam has heavy tails, and with  $q < 1$  it is more parabolic. The results show the  $q$ -parameter as the tails are shaved in V.

Figure 5 shows how the vertical and horizontal profiles change with shaving at the  $3Q_y$  resonance at the maximum sextupoles excitation of 40 A, (corresponding to  $k_2 = 0.18 \text{ m}^{-3}$ ). In V, the beam has large tails at 2% shaving, and when 34% of the intensity is shaved, the beam is more parabolic. In H, the beam is close to Gaussian at 2% shaving, and remains unaffected even when 34% of the intensity is shaved (in V), i. e. the profile is unaffected w.r.t intensity. Meaning, the amplitude of the particles in the vertical tails are not dependent in H, they are independently distributed.

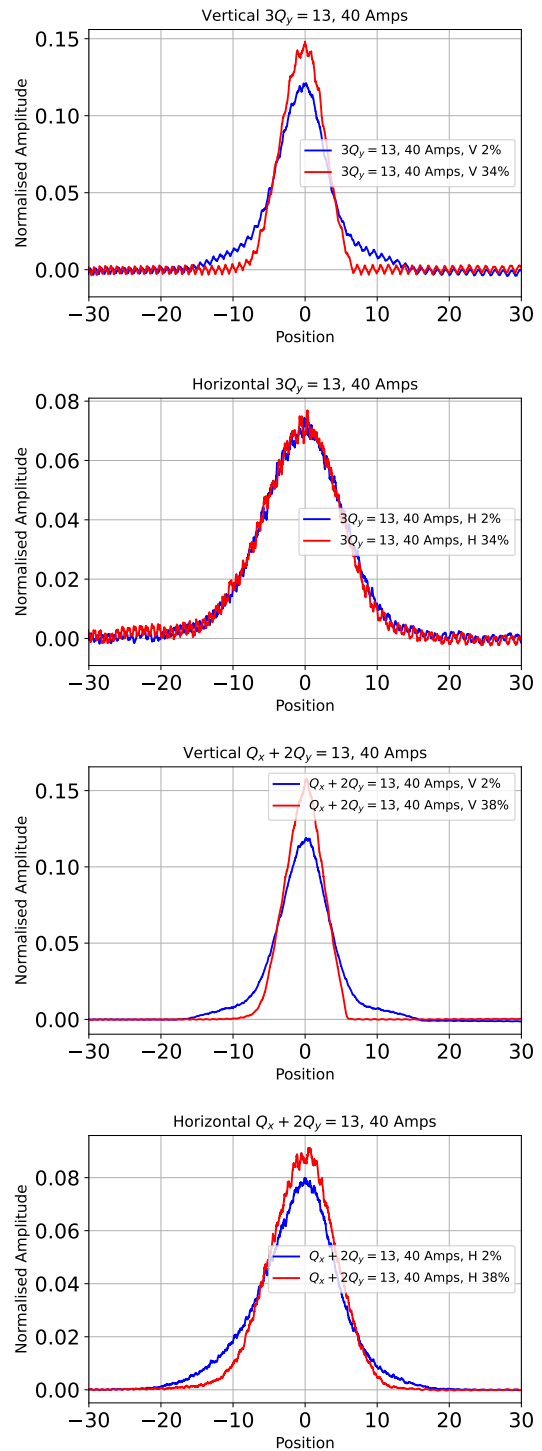


Figure 5: The profile change in H and V under vertical shaving, for the  $3Q_y$  resonance (top two plots) and the  $Q_x + 2Q_y$  resonance (bottom two plots). The profiles are normalised to their area for better comparison.

There is an asymmetry in the profiles, due to the Coulomb scattering of the beam particles on the wire [16, 17]. Figure 6 aggregates results for the  $3Q_y$  measurement. Increasing the resonance excitation increases the initial  $q$ -parameter in the V plane ( $q_V$ ), i. e. the tails are more populated. The initial

Content from this work may be used under the terms of the CC-BY-4.0 licence © 2023. Any distribution of this work must maintain attribution to the author(s), title of the work, publisher, and DOI

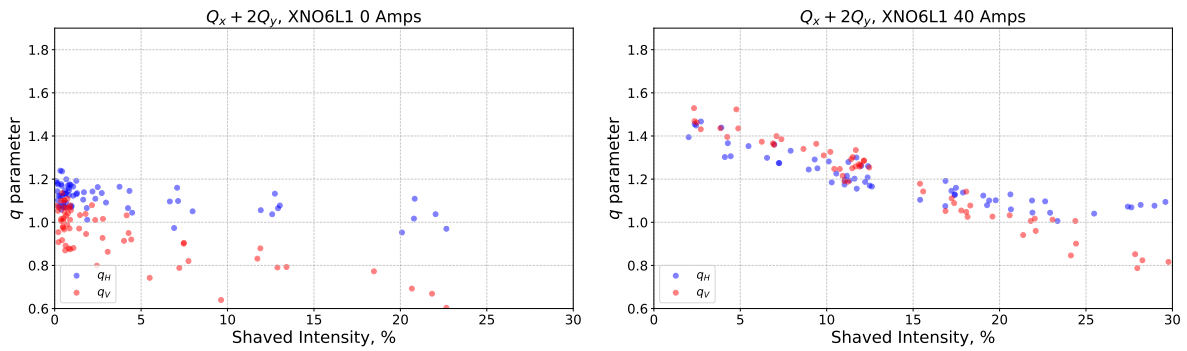


Figure 6: Aggregated results for the  $3Q_y = 13$  resonance showing how the  $q$ -parameter is changing in the H and V plane with shaving in the V plane.

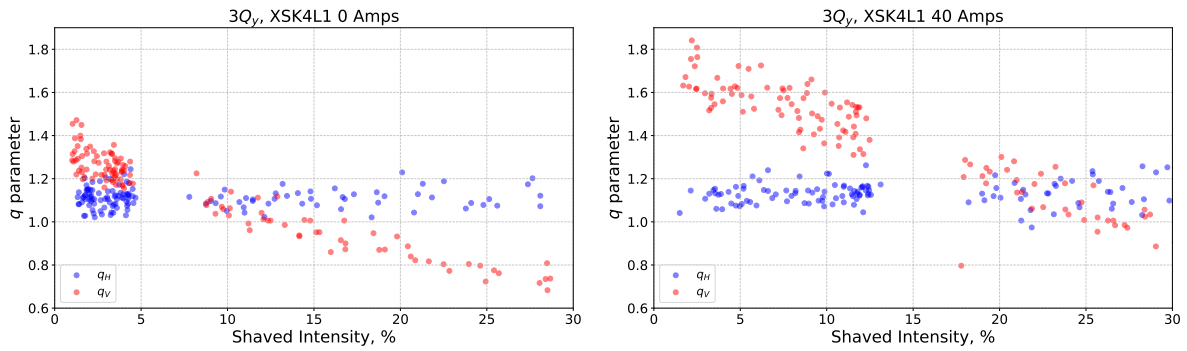


Figure 7: Results for the  $Q_x + 2Q_y = 13$  resonance showing how the  $q$ -parameter is changing in the H and V plane with shaving in the V plane.

$q_H$  is unchanged with excitation, as the resonance is purely vertical. Shaving the tail in V, the  $q$ -parameter decreases in V for all amplifications while  $q_H$  remains constant.

For  $Q_x + 2Q_y = 13$ , there is a different correction scheme used, as the working point is in a different location. Thus, a different powering is used on the corrector sextupole and octupolar magnets to compensate the resonances. With increasing excitation, the halo was further populated in both V and H. As the beam is shaved in V,  $q_V$  is reduced, but so is  $q_H$ , as shown in Fig. 7. This is also observed more visually in the wire scanner profiles shown in Fig. 5. In V, the tails are removed by the shaving. In H the profile is changed via shaving in V, with particles removed at the tails, meaning high amplitude particles in V are more likely to have high amplitudes in H.

## DISCUSSION

With the artificially excited machine resonances in these measurements a clear statistical dependence between the transverse planes was observed in the case of the 2D resonance. In operational conditions in the PSB, many resonances are crossed due to the large space charge tune-spread and the dynamic working point evolution. This could induce such a statistical dependence via 2D halo population if resonances are not perfectly corrected. Long term tracking simulations will provide further insight on this aspect. It is hypothesised that such a statistical dependence could be

passed along the injectors. In fact, it was observed in the SPS that shaving in V changed the profiles in both planes [18] during studies on tail population. Furthermore, if there is large dependence between the transverse planes in the LHC, then it affects the luminosity calculation, as the calculation assumes independent distributions in the  $x$ - $y$ . Calculations are needed to estimate the effect that dependent heavy tailed beams would have on the luminosity calculation, as was done for the near Gaussian case [9].

## CONCLUSION

Reconstructing the full beam distribution from a given beam profile is ambiguous, and it depends on the physical mechanism the beam has seen as to whether there are correlations between planes. In the PSB, two different types of distributions are generated, under 1D and 2D coupled resonances, the latter of which show to introduce dependence in the transverse planes. Long-term tracking simulations can be used to validate the PSB experimental results. It is still unclear whether, under normal operational scenarios, this effect is generated and transferred along the injector chain up to the LHC.

## ACKNOWLEDGEMENTS

The authors would like to thank the PSB operations teams.



## REFERENCES

- [1] S. Papadopoulou, F. Antoniou, T. Argyropoulos, M. Fitterer, M. Hostettler, and Y. Papaphilippou, “Modelling and measurements of bunch profiles at the LHC,” *J. Phys.: Conf. Ser.*, vol. 874, p. 012 008, 2017.  
doi:10.1088/1742-6596/874/1/012008
- [2] F. Asvesta, “Characterization of Transverse Profiles Along the LHC Injector Chain at CERN,” in *Proc. IPAC’23*, Venezia, Italy, May 2023, pp. 3490–3493.  
doi:10.18429/JACoW-IPAC2023-WEPL158
- [3] N. H. Abel, “Oeuvres Completes,” 1881.
- [4] R. Bracewell, *The Fourier Transform and Its Applications*. 3rd ed., McGraw-Hill, 1999.
- [5] Wikipedia contributors, “Q-Gaussian distribution,” *Wikipedia, The Free Encyclopedia*, 2022, accessed 30-March-2023. [https://en.wikipedia.org/w/index.php?title=Q-Gaussian\\_distribution&oldid=1123355647](https://en.wikipedia.org/w/index.php?title=Q-Gaussian_distribution&oldid=1123355647)
- [6] G. Box and M. Muller, “A Note on the Generation of Random Normal Deviates,” *Ann. Math. Statist.*, vol. 29, pp. 610–611, 1958. doi:10.1214/aoms/1177706645
- [7] Y. Batygin, “Particle-in-cell code BEAMPATH for beam dynamics simulations in linear accelerators and beamlines,” *Nucl. Instrum. Meth. A*, vol. 539, pp. 455–489, 2005.  
doi:10.1016/j.nima.2004.10.029
- [8] S. Papadopoulou, F. Antoniou, T. Argyropoulos, M. Hostettler, Y. Papaphilippou, and G. Trad, “Impact of non-Gaussian beam profiles in the performance of hadron colliders,” *Phys. Rev. Accel. Beams*, vol. 23, p. 101 004, 2020.  
doi:10.1103/PhysRevAccelBeams.23.101004
- [9] ATLAS Collaboration, “Luminosity determination in pp collisions at  $\sqrt{s} = 8$  TeV using the ATLAS detector at the LHC,” *Eur. Phys. J. C*, vol. 76, p. 653, 2016.  
doi:10.1140/epjc/s10052-016-4466-1
- [10] G. Franchetti and F. Schmidt, “Extending the Nonlinear-Beam-Dynamics Concept of 1D Fixed Points to 2D Fixed Lines,” *Phys. Rev. Lett.*, vol. 114, p. 234 801, 2015.  
doi:10.1103/PhysRevLett.114.234801
- [11] G. Franchetti, S. Gilardoni, A. Huschauer, F. Schmidt, and R. Wasef, “Space charge effects on the third order coupled resonance,” *Phys. Rev. Accel. Beams*, vol. 20, p. 081 006, 2017. doi:10.1103/PhysRevAccelBeams.20.081006
- [12] F. Asvesta *et al.*, “Resonance Compensation for High Intensity and High Brightness Beams in the CERN PSB,” in *Proc. HB’21*, Batavia, IL, USA, Oct. 2021, pp. 40–45.  
doi:10.18429/JACoW-HB2021-MOP06
- [13] F. Asvesta and H. Bartosik, “Resonance Driving Terms From Space Charge Potential,” CERN, Geneva, Switzerland, Rep. CERN-ACC-NOTE-2019-0046, 2019. <http://cds.cern.ch/record/2696190>
- [14] T. Prebibaj *et al.*, “Injection Chicane Beta-Beating Correction for Enhancing the Brightness of the CERN PSB Beams,” in *Proc. HB’21*, Batavia, IL, USA, Oct. 2021, pp. 112–117.  
doi:10.18429/JACoW-HB2021-MOP18
- [15] S. Hancock, M. Lindroos, and S. Koscielniak, “Longitudinal phase space tomography with space charge,” *Phys. Rev. Spec. Top. Accel. Beams*, vol. 3, p. 124 202, 2000.  
doi:10.1103/PhysRevSTAB.3.124202
- [16] F. Roncarolo, “Accuracy of the Transverse Emittance Measurements of the CERN Large Hadron Collider,” PhD thesis, Politecnico di Milano, Italy, 2005. <https://cds.cern.ch/record/1481835>
- [17] T. Prebibaj *et al.*, “Characterization of the Vertical Beam Tails in the CERN PS Booster,” in *Proc. IPAC’22*, Bangkok, Thailand, Jun. 2022, pp. 218–221.  
doi:10.18429/JACoW-IPAC2022-MOPOST057
- [18] I. Mases and E. de la Fuente, “Emittance and tails studies in the SPS,” CERN, Geneva, Switzerland, INC Section Meeting 54, 2022.